IEEE Access
Multidisciplinary | Rapid Review | Open Access Journal

Received November 22, 2018, accepted December 12, 2018, date of publication December 28, 2018,
date of current version January 23, 2019.

Digital Object Identifier 10.1109/ACCESS.2018.2890086

Cooperative Game Theory-Based Optimal Angular Momentum Management of Hybrid Attitude Control Actuator

YUNHUA WU[1,2], MOHONG ZHENG[1], MENGJIE HE[1], DAWEI ZHANG[3], WEI HE[4], BING HUA[1], ZHIMING CHEN[1], AND FENG WANG[2]

[1]School of Astronautics, Nanjing University of Aeronautics and Astronautics, Nanjing 210016, China
[2]School of Astronautics, Harbin Institute of Technology, Harbin 150010, China
[3]Institute of Spacecraft System Engineering, CAST, Beijing 100094, China
[4]Shanghai Electro-Mechanical Engineering Institute, Shanghai 201109, China

Corresponding author: Yunhua Wu (yunhuawu@nuaa.edu.cn)

This work was supported in part by the National Key Research and Development Plan under Grant 2016YFB0500901, and in part by the Open Fund of National Defense Key Discipline Laboratory of Micro-Spacecraft Technology under Grant HIT.KLOF.MST.201705.

ABSTRACT The next-generation space missions, such as the space moving target tracking mission and the agile attitude maneuvering mission and so on, propose a high requirement on spacecraft attitude control system. For such missions, hybrid attitude control actuators consisting of control moment gyro and reaction wheel, which can not only offer large control torque but also achieve high control precision, is the best alternative choice. For this hybrid actuator system, the angular momentum management is vital. To handle the momentum management problem, an optimal angular momentum strategy based on cooperative game theory is proposed. The cooperative game model is constructed according to the quadratic programming problem to achieve the minimization of control moment gyro gimbal angular speed and reaction wheel angular acceleration. The proposed cooperative game theory steering logic has overcome the control moment gyro singular problem and reaction wheel saturation problem of the hybrid system. In addition, the energy cost of the hybrid actuator system is reduced. Five groups of simulation scenarios are carried out to demonstrate the effectiveness of the proposed steering logic.

INDEX TERMS Agile attitude control, hybrid actuator, cooperative game theory, quadratic programming problem, angular momentum management.

I. INTRODUCTION

With the complexity of space missions adding, the attitude agile maneuvering and attitude dynamic tracking has put forward a stringent requirement on the spacecraft attitude control system [1]. For example, the Pleiades high-resolution imaging satellite requires approximately 3 deg/sec slew rate for rapid rotational maneuver [2]. The XSS-10 micro-satellite requires the attitude control system to provide rapid rotational maneuverability and tracking capability with high precision [3]. Agile maneuvering and attitude tracking require the attitude control actuator can output large attitude control torque with higher accuracy.

The most common attitude control actuators include thruster, RW (Reaction Wheel), CMG (Control Moment Gyros), magnetic torquer, and so on, each of which has its own limitations and can hardly meet the demands of the above space missions. For example, thruster consumes valuable propellant and has low control accuracy [4]. The output of RW is relatively small to meet the agility requirement of the above missions [5]. The torque amplification capability makes CMG a good choice for space missions with agile maneuvering requirement; however, the inherent singular problem prevents its further application [6]. Magnetic torquer with small output is usually used for micro-satellite [7], as well as RW desaturation.

Hybrid actuator is the best alternative actuator for agile maneuvering and attitude tracking missions, and has been taken into consideration in many researches [8]–[12]. The combination of RW and thruster was studied by Ye *et al.* [8] for large angle rapid reorientation. The combination of RW and magnetic torquer was presented by Li *et al.* [9] for a CubeSat. The implementations of hybrid actuator consisting of CMG and RW were demonstrated in target tracking [10], on-orbit servicing [11] and agile maneuvering [12].

Since CMG cluster would trap into a singularity state and RW tends to be saturated, the control torque cannot be guaranteed for the above situation. Therefore, how to overcome the CMG singularity and RW saturation problem through the cooperation between the CMG and RW is the major problem for the implementation of the hybrid actuator. Wu *et al.* [13] proposed a null motion steering logic to operate the CMG+RW system. Doupe and Swenson [14] evaluated the CMG+RW system by analytical simulations and hardware experiments, and ensured the CMG gimbal angles travel the shortest path through a closed-loop control scheme. Cao and Wu [15] developed a torque allocation method to allow a smooth switch between CMG and RW. Although the above researches have solved the implementation problem of hybrid actuator, the energy consumption or angular momentum has not been considered.

This paper aims to achieve angular momentum optimal management by using cooperative game theory for the CMG+RW hybrid system. To guarantee the large control torque with high precision, the cooperative game theory steering logic proposed can avoid the CMG singularity and RW saturation and reduce energy cost by momentum management strategy. The remainder of this work is outlined as follows. Section 2 briefly introduces the hybrid actuator configuration and attitude dynamics. Followed by a quadratic programming problem in section 3. Section 4 proposes the cooperative game theory steering logic for the hybrid actuator system. Numerical simulations are carried out in section 5 to demonstrate the efficiency of the proposed steering logic. Finally, section 6 concludes the entire work of this research.

II. HYBRID ACTUATOR AND ATTITUDE DYNAMICS

CMG+RW system is involved in the advantages of CMG and RW and these make it suitable for agile spacecraft. A hybrid actuator system consisting of CMG and RW is constructed and attitude dynamics is presented in this section.

A. ATTITUDE KINEMATICS AND DYNAMICS

First, four coordinate frames are defined as follows:

Inertial Frame $OX_IY_IZ_I$: Its origin is located at the center of mass of the Earth. The OX_I axis points to the equinox, and the OZ_I axis is along the Earth's rotation axis.

Orbit Reference Frame $OX_OY_OZ_O$: Its origin is located at the center of mass of the spacecraft. The OY_O axis is along the anti-symmetric direction of the orbit momentum, and the OZ_O axis points to the Earth's center.

Spacecraft Body Frame $OX_BY_BZ_B$: Its origin is located at the center of mass of the spacecraft, and the three axes of the frame coincide with the three major axes of the spacecraft.

Desired Imaging Frame $OX_cY_cZ_c$: Its origin is located at the center of mass of the spacecraft. The OZ_c axis points to the target and the OY_c axis is along the OY_b axis.

Please note that all the above coordinate frames are right-handed frames.

The spacecraft attitude kinematic model is represented by quaternion $\boldsymbol{Q} = [q_0, \ \boldsymbol{q}^{\mathrm{T}}]^{\mathrm{T}}$, attitude angular velocity $\boldsymbol{\omega} = [\omega_x, \ \omega_y, \ \omega_z]^{\mathrm{T}}$ as,

$$\dot{\boldsymbol{Q}} = \frac{1}{2}\begin{bmatrix} -\boldsymbol{q}^{\mathrm{T}} \\ q_0\boldsymbol{E}_3 + \boldsymbol{q}^{\times} \end{bmatrix}\boldsymbol{\omega} \tag{1}$$

where, q_0 is the scalar part and $\boldsymbol{q} = [q_1, q_2, q_3]^{\mathrm{T}}$ is the vector part of quaternion, $\boldsymbol{E}_3 \in \mathrm{R}^{3\times3}$ denotes an identity matrix, and $\boldsymbol{\omega}$ is the angular velocity of the Spacecraft Body Frame with respect to the Inertial Frame and expressed in the Spacecraft Body Frame. Similarly, the error quaternion $\boldsymbol{Q}_e = [q_{e0}, \ \boldsymbol{q}_e^{\mathrm{T}}]^{\mathrm{T}}$ is calculated by,

$$\dot{\boldsymbol{Q}}_e = \frac{1}{2}\begin{bmatrix} -\boldsymbol{q}_e^{\mathrm{T}} \\ q_{e0}\boldsymbol{E}_3 + \boldsymbol{q}_e^{\times} \end{bmatrix}\boldsymbol{\omega}_e \tag{2}$$

where $\boldsymbol{\omega}_e$ is the error attitude angular velocity expressed in Spacecraft Body Frame.

The angular momentum of the whole spacecraft is $\boldsymbol{H} = \boldsymbol{J}\boldsymbol{\omega} + \boldsymbol{h}$, in which $\boldsymbol{J}$ is the moment of inertia of the spacecraft, and $\boldsymbol{h}$ is the momentum of the actuator. The dynamic model of the spacecraft can be written as,

$$\boldsymbol{M} = \frac{d\boldsymbol{H}}{dt} = \boldsymbol{J}\dot{\boldsymbol{\omega}} + \dot{\boldsymbol{h}} + \boldsymbol{\omega} \times (\boldsymbol{J}\boldsymbol{\omega} + \boldsymbol{h}) \tag{3}$$

where $\boldsymbol{M}$ is the sum of disturbance and control torque.

B. HYBIRD ACTUATOR SYSTEM CONFIGURATION

CMG+RW can generate large control torque with high precision, but the worst situation in using CMG and RW is CMG saturation singularity and RW saturation problem. However, this case can be solved by desaturation with other actuators such as magnetic rods, and therefore this case is not the focus of this paper and is not considered. In this paper, CMG hyperbolic and elliptic singularities and RW saturation will be overcome simultaneously through the cooperation between the two sets of actuators.

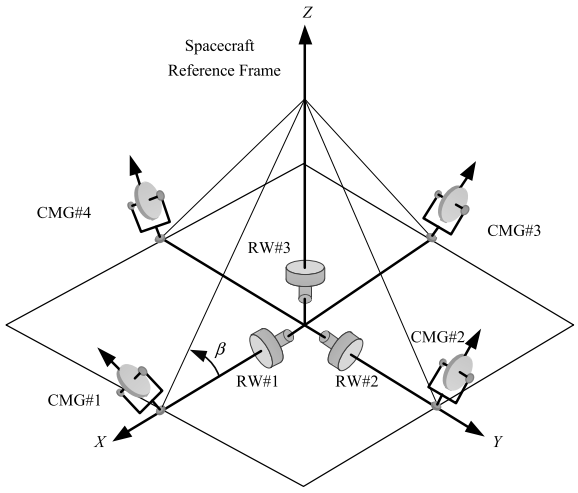

FIGURE 1. Hybrid actuator configuration.

The hybrid actuator configuration contains a pyramid CMG cluster [16], [17] with skew angle β and three orthogonal RWs, as shown in Fig. 1 [13]. Let $\boldsymbol{\alpha} = [\alpha_1, \alpha_2, \alpha_3, \alpha_4]^{\mathrm{T}}$

be the gimbal angles of the CMG cluster and $\boldsymbol{\Omega}_{\mathrm{RW}} = [\Omega_{\mathrm{RW1}}, \Omega_{\mathrm{RW2}}, \Omega_{\mathrm{RW3}}]^{\mathrm{T}}$ be the angular speeds of each RW. Therefore, $\boldsymbol{h}$ can be calculated as (4), as shown at the bottom of this page, where $\mathrm{c}(\beta) \equiv \cos(\beta)$, $\mathrm{s}(\beta) \equiv \sin(\beta)$, $\mathrm{s}(\alpha_i) \equiv \sin(\alpha_i)$, and $\mathrm{c}(\alpha_i) \equiv \cos(\alpha_i)$. $\boldsymbol{h}_{\mathrm{CMG}}$ and $\boldsymbol{h}_{\mathrm{RW}}$ are the momentums of CMG and RW, respectively, $\boldsymbol{A}_{\mathrm{CMG},\,i}$ is a matrix consisting of the i^{th} CMG flywheel momentum directions, and $\boldsymbol{J}_{\mathrm{RW}}$ is the moment of inertia matrix of the RW,

$$\begin{aligned}
\boldsymbol{A}_{\mathrm{CMG},\,1} &= \begin{bmatrix} -c(\beta)s(\alpha_1) & c(\alpha_1) & s(\beta)s(\alpha_1) \end{bmatrix}^{\mathrm{T}} \\
\boldsymbol{A}_{\mathrm{CMG},\,2} &= \begin{bmatrix} -c(\alpha_2) & -c(\beta)s(\alpha_2) & s(\beta)s(\alpha_2) \end{bmatrix}^{\mathrm{T}} \\
\boldsymbol{A}_{\mathrm{CMG},\,3} &= \begin{bmatrix} c(\beta)s(\alpha_3) & -c(\alpha_3) & s(\beta)s(\alpha_3) \end{bmatrix}^{\mathrm{T}} \\
\boldsymbol{A}_{\mathrm{CMG},\,4} &= \begin{bmatrix} c(\alpha_4) & c(\beta)c(\alpha_4) & s(\beta)s(\alpha_4) \end{bmatrix}^{\mathrm{T}}
\end{aligned}$$

The time derivative of (4) is,

$$\dot{\boldsymbol{h}} = h_0 \dot{\boldsymbol{A}}_{\mathrm{CMG}} + \boldsymbol{J}_{\mathrm{RW}} \dot{\boldsymbol{\Omega}}_{\mathrm{RW}} = \boldsymbol{A}\dot{\boldsymbol{\delta}} \tag{5}$$

where $\dot{\boldsymbol{\delta}} = [\dot{\boldsymbol{\alpha}},\ \dot{\boldsymbol{\Omega}}_{\mathrm{RW}}]^{\mathrm{T}}$ is a set of the CMG gimbal angular speed and RW angular acceleration and $\boldsymbol{A}$ is the system matrix of CMG+RW system,

$$\boldsymbol{A} = \begin{bmatrix} h_0 \begin{bmatrix} -\mathrm{c}(\beta)\mathrm{c}(\alpha_1) & -s(\alpha_1) & s(\beta)\mathrm{c}(\alpha_1) \\ s(\alpha_2) & -c(\beta)\mathrm{c}(\alpha_2) & s(\beta)\mathrm{c}(\alpha_2) \\ c(\beta)c(\alpha_3) & s(\alpha_3) & s(\beta)\mathrm{c}(\alpha_3) \\ -s(\alpha_4) & c(\beta)c(\alpha_4) & s(\beta)\mathrm{c}(\alpha_4) \end{bmatrix}^{\mathrm{T}} \\ \begin{matrix} J_{\mathrm{RW1}} & 0 & 0 \\ 0 & J_{\mathrm{RW2}} & 0 \\ 0 & 0 & J_{\mathrm{RW3}} \end{matrix} \end{bmatrix}$$

C. CMG SINGULARITY

When the CMG cluster traps into a singularity state, the output torque and the control torque are orthogonal. Meanwhile, the Jacobian matrix $\boldsymbol{J}_{\mathrm{a}}$ satisfies,

$$\mathrm{rank}(\boldsymbol{J}_{\mathrm{a}}) < 3 \quad \text{and} \quad \det\left(\boldsymbol{J}_{\mathrm{a}}\boldsymbol{J}_{\mathrm{a}}^{\mathrm{T}}\right) = 0$$

where,

$$\boldsymbol{J}_{\mathrm{a}} = \begin{bmatrix} -\mathrm{c}(\beta)\mathrm{c}(\alpha_1) & -s(\alpha_1) & s(\beta)\mathrm{c}(\alpha_1) \\ s(\alpha_2) & -c(\beta)\mathrm{c}(\alpha_2) & s(\beta)\mathrm{c}(\alpha_2) \\ c(\beta)c(\alpha_3) & s(\alpha_3) & s(\beta)\mathrm{c}(\alpha_3) \\ -s(\alpha_4) & c(\beta)c(\alpha_4) & s(\beta)\mathrm{c}(\alpha_4) \end{bmatrix}^{\mathrm{T}}$$

The singular momentum can be calculated by [17],

$$\boldsymbol{h}_{\mathrm{s}i} = \varepsilon_i \frac{\left(\boldsymbol{g}_i \times \boldsymbol{u}_{\mathrm{s}}\right) \times \boldsymbol{g}_i}{\left|\boldsymbol{g}_i \times \boldsymbol{u}_{\mathrm{s}}\right|} \tag{6}$$

where $\boldsymbol{h}_{\mathrm{s}i}$ is the singular momentum of CMG, $\varepsilon_i = \pm 1$, $\boldsymbol{g}_i$ is the gimbal axis and $\boldsymbol{u}_{\mathrm{s}}$ is an arbitrary vector in three-dimensional space.

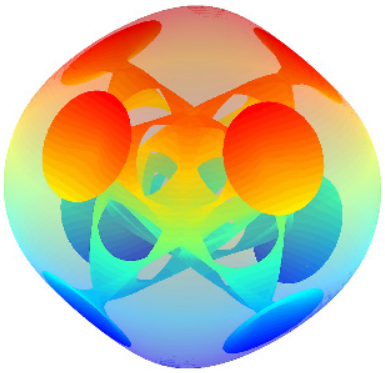

FIGURE 2. Singular surface of pyramid CMG cluster.

The singular momentum surface of a pyramid CMG cluster is shown in Fig. 2 [13], including 0H singular surface, 2H singular surface and 4H singular surface. It is clear that the external surface is the momentum envelope where the momentum approaches the maximum. The singular momentum surface is symmetrical due to the symmetrical structure of the pyramid CMG cluster.

The singularity index S_{CMG} is used to determine whether the CMG cluster traps into a singularity state,

$$S_{\mathrm{CMG}} = \frac{\det\left(\boldsymbol{J}_{\mathrm{a}}\boldsymbol{J}_{\mathrm{a}}^{\mathrm{T}}\right)}{\left[\det\left(\boldsymbol{J}_{\mathrm{a}}\boldsymbol{J}_{\mathrm{a}}^{\mathrm{T}}\right)\right]_{\max}} \in [0, 1] \tag{7}$$

where, $\left[\det\left(\boldsymbol{J}_{\mathrm{a}}\boldsymbol{J}_{\mathrm{a}}^{\mathrm{T}}\right)\right]_{\max}$ is the maximum value of $\det\left(\boldsymbol{J}_{\mathrm{a}}\boldsymbol{J}_{\mathrm{a}}^{\mathrm{T}}\right)$ and its value depends on the configuration of CMG cluster. For the configuration used in the paper, $\left[\det\left(\boldsymbol{J}_{\mathrm{a}}\boldsymbol{J}_{\mathrm{a}}^{\mathrm{T}}\right)\right]_{\max} = 2.37$.

The singularity index S_{CMG} is used to identify whether the CMG traps into a singularity state and how far the CMG is from the singularity state. $S_{\mathrm{CMG}} = 0$ means CMG cluster traps into a singularity state. It is important to help to evaluate the effectiveness of the proposed steering logic.

III. QUADRATIC PROGRAMMING PROBLEM

The required attitude control torque for the agile maneuvering mission is represented as $\boldsymbol{u}_{\mathrm{c}} = [u_{\mathrm{c,x}},\ u_{\mathrm{c,y}},\ u_{\mathrm{c,z}}]^{\mathrm{T}}$. In order to manage and optimize momentum and to minimize the energy cost of the hybrid actuator, the following quadratic programming problem is considered,

$$\text{Minimize} \sum_{k=1}^{4} \dot{\alpha}_k^2 + \sum_{k=1}^{3} \dot{\Omega}_k^2 \tag{8a}$$

$$\text{Constraints } \boldsymbol{A}\dot{\boldsymbol{\delta}} = \boldsymbol{u}_{\mathrm{c}} \tag{8b}$$

$$\begin{aligned}
\boldsymbol{h} &= \boldsymbol{h}_{\mathrm{CMG}} + \boldsymbol{h}_{\mathrm{RW}} = h_0 \sum_{i=1}^{4} \boldsymbol{A}_{\mathrm{CMG},\,i} + \boldsymbol{J}_{\mathrm{RW}}\boldsymbol{\Omega}_{\mathrm{RW}} \\
&= \begin{bmatrix} h_0\left(-\mathrm{c}(\beta)s(\alpha_1) - c(\alpha_2) + c(\beta)s(\alpha_3) + c(\alpha_4)\right) + J_{\mathrm{RW1}}\Omega_{\mathrm{RW1}} \\ h_0\left(c(\alpha_1) - c(\beta)s(\alpha_2) - c(\alpha_3) + c(\beta)s(\alpha_4)\right) + J_{\mathrm{RW2}}\Omega_{\mathrm{RW2}} \\ h_0 s(\beta)\left(s(\alpha_1) + s(\alpha_2) + s(\alpha_3) + s(\alpha_4)\right) + J_{\mathrm{RW3}}\Omega_{\mathrm{RW3}} \end{bmatrix}
\end{aligned} \tag{4}$$

where $\dot{\boldsymbol{\alpha}} = [\dot{\alpha}_1,\ \dot{\alpha}_2,\ \dot{\alpha}_3,\ \dot{\alpha}_4]^{\mathrm{T}}$ and $\dot{\boldsymbol{\Omega}} = [\dot{\Omega}_1,\ \dot{\Omega}_2,\ \dot{\Omega}_3]^{\mathrm{T}}$ are the CMG gimbal angular speed and RW angular acceleration, respectively.

It can be converted to the minimization problem of $L(\dot{\boldsymbol{\alpha}},\ \dot{\boldsymbol{\Omega}})$,

$$L(\dot{\boldsymbol{\alpha}}, \dot{\boldsymbol{\Omega}}) = \sum_{k=1}^{4} \dot{\alpha}_k^2 + \sum_{k}^{3} \dot{\Omega}_k^2 \tag{9a}$$

Subjected to,

$$f(\dot{\boldsymbol{\alpha}}, \dot{\boldsymbol{\Omega}}) = \begin{bmatrix} f_1(\dot{\boldsymbol{\alpha}}, \dot{\boldsymbol{\Omega}}) \\ f_2(\dot{\boldsymbol{\alpha}}, \dot{\boldsymbol{\Omega}}) \\ f_3(\dot{\boldsymbol{\alpha}}, \dot{\boldsymbol{\Omega}}) \end{bmatrix} = 0 \tag{9b}$$

where,

$$\begin{aligned} f_1(\dot{\boldsymbol{\alpha}}, \dot{\boldsymbol{\Omega}}) &= A_{11}\dot{\alpha}_1 + A_{12}\dot{\alpha}_2 + A_{13}\dot{\alpha}_3 + A_{14}\dot{\alpha}_4 \\ &\quad + A_{15}\dot{\Omega}_1 + A_{16}\dot{\Omega}_2 + A_{17}\dot{\Omega}_3 - u_{\mathrm{c,x}} \qquad (10a) \\ f_2(\dot{\boldsymbol{\alpha}}, \dot{\boldsymbol{\Omega}}) &= A_{21}\dot{\alpha}_1 + A_{22}\dot{\alpha}_2 + A_{23}\dot{\alpha}_3 + A_{24}\dot{\alpha}_4 \\ &\quad + A_{25}\dot{\Omega}_1 + A_{26}\dot{\Omega}_2 + A_{27}\dot{\Omega}_3 - u_{\mathrm{c,y}} \qquad (10b) \\ f_3(\dot{\boldsymbol{\alpha}}, \dot{\boldsymbol{\Omega}}) &= A_{31}\dot{\alpha}_1 + A_{32}\dot{\alpha}_2 + A_{33}\dot{\alpha}_3 + A_{34}\dot{\alpha}_4 \\ &\quad + A_{35}\dot{\Omega}_1 + A_{36}\dot{\Omega}_2 + A_{37}\dot{\Omega}_3 - u_{\mathrm{c,z}} \qquad (10c) \end{aligned}$$

$A_{ij} = \boldsymbol{A}(i, j)$ is the element of the Jacobian matrix of CMG+RW system in line i and column j. Let,

$$\begin{aligned} H(\dot{\boldsymbol{\alpha}}, \dot{\boldsymbol{\Omega}}, \boldsymbol{\lambda}) &= L(\dot{\boldsymbol{\alpha}}, \dot{\boldsymbol{\Omega}}) + \boldsymbol{\lambda}^{\mathrm{T}} f(\dot{\boldsymbol{\alpha}}, \dot{\boldsymbol{\Omega}}) \\ &= L(\dot{\boldsymbol{\alpha}}, \dot{\boldsymbol{\Omega}}) + \lambda_1 f_1(\dot{\boldsymbol{\alpha}}, \dot{\boldsymbol{\Omega}}) \\ &\quad + \lambda_2 f_2(\dot{\boldsymbol{\alpha}}, \dot{\boldsymbol{\Omega}}) + \lambda_3 f_3(\dot{\boldsymbol{\alpha}}, \dot{\boldsymbol{\Omega}}) \end{aligned} \tag{11}$$

where $\boldsymbol{\lambda} = [\lambda_1,\ \lambda_2,\ \lambda_3]^{\mathrm{T}}$. We obtain,

$$\frac{\partial H(\dot{\boldsymbol{\alpha}}, \dot{\boldsymbol{\Omega}}, \boldsymbol{\lambda})}{\partial \dot{\alpha}_k} = 0, \quad k = 1, 2, 3, 4 \tag{12a}$$

$$\frac{\partial H(\dot{\boldsymbol{\alpha}}, \dot{\boldsymbol{\Omega}}, \boldsymbol{\lambda})}{\partial \dot{\Omega}_k} = 0, \quad k = 1, 2, 3 \tag{12b}$$

Substituting (12a) and (12b), the time derivative of (11) is written as,

$$\begin{aligned} &\frac{\partial H(\dot{\boldsymbol{\alpha}}, \dot{\boldsymbol{\Omega}}, \boldsymbol{\lambda})}{\partial \dot{\alpha}_1} = 2\dot{\alpha}_1 + \lambda_1 A_{11} + \lambda_2 A_{21} + \lambda_3 A_{31} = 0 \\ &\qquad\qquad \vdots \\ &\frac{\partial H(\dot{\boldsymbol{\alpha}}, \dot{\boldsymbol{\Omega}}, \boldsymbol{\lambda})}{\partial \dot{\alpha}_4} = 2\dot{\alpha}_4 + \lambda_1 A_{14} + \lambda_2 A_{24} + \lambda_3 A_{34} = 0 \qquad (13a) \\ &\frac{\partial H(\dot{\boldsymbol{\alpha}}, \dot{\boldsymbol{\Omega}}, \boldsymbol{\lambda})}{\partial \dot{\Omega}_1} = 2\dot{\Omega}_1 + \lambda_1 A_{15} + \lambda_2 A_{25} + \lambda_3 A_{35} = 0 \\ &\qquad\qquad \vdots \\ &\frac{\partial H(\dot{\boldsymbol{\alpha}}, \dot{\boldsymbol{\Omega}}, \boldsymbol{\lambda})}{\partial \dot{\Omega}_3} = 2\dot{\Omega}_3 + \lambda_1 A_{17} + \lambda_2 A_{27} + \lambda_3 A_{37} = 0 \qquad (13b) \end{aligned}$$

Therefore, we have,

$$\dot{\alpha}_k = -\frac{1}{2}\sum_{\mathrm{i}=1}^{3} \lambda_i A_{ik}, \quad k = 1, 2, 3, 4 \tag{14a}$$

$$\dot{\Omega}_k = -\frac{1}{2}\sum_{\mathrm{i}=1}^{3} \lambda_i A_{im}, \quad k = 1, 2, 3,\ m = k + 4 \tag{14b}$$

The CMG singularity problem will be changed to the CMG+RW system singularity problem according to (14a)- (14b).

Substituting (14a) and (14b) into (9), we have,

$$\begin{aligned} L(\dot{\boldsymbol{\alpha}}, \dot{\boldsymbol{\Omega}}) &= \sum_{k=1}^{4} \dot{\alpha}_k^2 + \sum_{k}^{3} \dot{\Omega}_k^2 \\ &= \frac{1}{4}\left(\sum_{\mathrm{i}=1}^{3} \lambda_i A_{i1}\right)^2 + \frac{1}{4}\left(\sum_{\mathrm{i}=1}^{3} \lambda_i A_{i2}\right)^2 \\ &\quad + \frac{1}{4}\left(\sum_{\mathrm{i}=1}^{3} \lambda_i A_{i3}\right)^2 + \frac{1}{4}\left(\sum_{\mathrm{i}=1}^{3} \lambda_i A_{i4}\right)^2 \\ &\quad + \frac{1}{4}\left(\sum_{\mathrm{i}=1}^{3} \lambda_i A_{i5}\right)^2 + \frac{1}{4}\left(\sum_{\mathrm{i}=1}^{3} \lambda_i A_{i5}\right)^2 \\ &\quad + \frac{1}{4}\left(\sum_{\mathrm{i}=1}^{3} \lambda_i A_{i6}\right)^2 \\ &= -\frac{1}{2}a_1\lambda_1^2 - \frac{1}{2}a_2\lambda_2^2 - \frac{1}{2}a_3\lambda_3^3 - a_{12}\lambda_1\lambda_2 \\ &\quad - a_{13}\lambda_1\lambda_3 - a_{23}\lambda_2\lambda_3 \end{aligned} \tag{15a}$$

$$\begin{aligned} f(\dot{\boldsymbol{\alpha}}, \dot{\boldsymbol{\Omega}}) &= f(\boldsymbol{A}, \boldsymbol{\lambda}) \\ &= \begin{bmatrix} a_1 & a_{12} & a_{13} \\ a_{12} & a_2 & a_{23} \\ a_{13} & a_{23} & a_3 \end{bmatrix} \begin{bmatrix} \lambda_1 \\ \lambda_2 \\ \lambda_3 \end{bmatrix} - \begin{bmatrix} u_{\mathrm{c,x}} \\ u_{\mathrm{c,y}} \\ u_{\mathrm{c,z}} \end{bmatrix} \end{aligned} \tag{15b}$$

where $f(\boldsymbol{A}, \boldsymbol{\lambda}) \leq 0$. The elements $a_i (i = 1, 2, 3)$ and $a_{ij} (i = 1, 2, 3; j = 1, 2, 3; i \neq j)$ are defined as,

$$a_i = -\frac{1}{2}\sum_{\mathrm{k}=1}^{7} A_{ik}^2, \quad i = 1, 2, 3 \tag{16a}$$

$$a_{ij} = -\frac{1}{2}\sum_{\mathrm{k}=1}^{7} A_{ik}A_{jk}, \quad i = 1, 2, 3;\ j = 1, 2, 3;\ i < j \tag{16b}$$

IV. COOPERATIVE GAME THEORY STEERING LOGIC

The cooperative game theory steering logic for CMG cluster only has been designed to overcome CMG singular problem [18], however, it is not efficient for all kinds of CMG singular problems. This paper proposes a hybrid actuator steering logic based on cooperative game theory to avoid the CMG singularity and RW saturation simultaneously. Weighted elements are presented as well to improve the iteration speed and accuracy. The energy cost of the hybrid actuator is reduced by optimizing the angular momentum of the hybrid system.

A. COOPERATIVE GAME MODEL

The cooperative game model is set as $G = \{N,\ V\}$, where V is real-value function and $N = \{1,\ 2,\ 3\}$ are players, including player 1, player 2, and player 3. In cooperative game, at least one player' gain increases and the other's gains are not compromised in cooperative game.

Suppose the strategy set of the player i is $\boldsymbol{D}_i$. A game situation $\boldsymbol{\lambda} = [\lambda_1,\ \lambda_2,\ \lambda_3]$ can be defined after all players choose a strategy satisfying $\left|f_j(\boldsymbol{A},\ \boldsymbol{\lambda})\right| \leq \varepsilon_D,\ j = 1,\ 2,\ 3$. The strategy $\boldsymbol{D}_i$ $(i = 1,\ 2,\ 3)$ is designed by,

$$\boldsymbol{D}_i = \left\{\lambda_i |\ \left|f_j(\boldsymbol{A},\ \boldsymbol{\lambda})\right| \leq \varepsilon_D,\ j = 1,\ 2,\ 3\right\} \quad i = 1,\ 2,\ 3$$

where ε_D is a small positive scalar. The strategy set $\boldsymbol{D}_i$ includes all feasible solutions λ_i of $\left|f_j(\boldsymbol{A},\ \boldsymbol{\lambda})\right| \leq \varepsilon_D$, meaning that the output torque $\boldsymbol{u}_{\mathrm{o}} = [u_{\mathrm{o,\,x}},\ u_{\mathrm{o,\,y}},\ u_{\mathrm{o,\,z}}]^{\mathrm{T}}$ satisfies that $\left|u_{\mathrm{o,\,x}} - u_{\mathrm{c,\,x}}\right| \leq \varepsilon_D$, $\left|u_{\mathrm{o,\,y}} - u_{\mathrm{c,\,y}}\right| \leq \varepsilon_D$ and $\left|u_{\mathrm{o,\,z}} - u_{\mathrm{c,\,z}}\right| \leq \varepsilon_D$. There existing an optimal strategy $\lambda_i^{\#} \in D_i$ satisfies the constraint $\left|f_j(\boldsymbol{A},\ \boldsymbol{\lambda})\right| \to 0$ and $\boldsymbol{u}_{\mathrm{o}} - \boldsymbol{u}_{\mathrm{c}} = 0$.

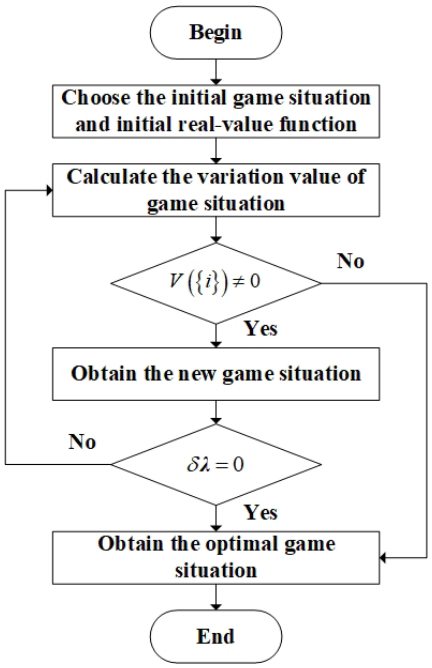

FIGURE 3. Flowchart of cooperative game.

As shown in Fig. 3, an initial game situation $\boldsymbol{\lambda} = [\lambda_1,\ \lambda_2,\ \lambda_3]$ is selected at the beginning of the game. A set of strategy variation value of game situation $\delta\boldsymbol{\lambda} = [\delta\lambda_1,\ \delta\lambda_2,\ \delta\lambda_3]$ will be generated in every negotiation, and the new game situation will be $\boldsymbol{\lambda} = \boldsymbol{\lambda} + \delta\boldsymbol{\lambda}$. Note that $\delta\boldsymbol{\lambda}$ should be set as $\delta\boldsymbol{\lambda} = \nu_\lambda[f(\boldsymbol{A}, \boldsymbol{\lambda})]$, and it satisfies that $\delta\boldsymbol{\lambda} \to 0$ as $\left|f_j(\boldsymbol{A},\ \boldsymbol{\lambda})\right| \to 0$. $\nu_\lambda[f(\boldsymbol{A}, \boldsymbol{\lambda})]$ is a function of $f(\boldsymbol{A}, \boldsymbol{\lambda})$ which should be design properly. The real-value function $V(\{i\})$ of λ_i is chosen as,

$$V(\{i\}) = \begin{cases} \dfrac{1}{3}(1 - \delta\lambda_i), & \delta\lambda_1 < \delta\lambda_1^- \text{ or } \delta\lambda_2 < \delta\lambda_2^- \\ & \text{or } \delta\lambda_3 < \delta\lambda_3^- \\ 0, & \delta\lambda_1 \geq \delta\lambda_1^- \text{ and } \delta\lambda_2 \geq \delta\lambda_2^- \\ & \text{and } \delta\lambda_3 \geq \delta\lambda_3^- \end{cases} \tag{17}$$

where $\delta\lambda_i^-$ is the strategy variation value of game situation in the previous negotiation.

To ensure at least one player's gain increases in every negotiation, at least one new strategy λ_i is closer to the $\lambda_i^{\#}$. If $\delta\lambda_i \geq \delta\lambda_i^-$ $(i = 1,\ 2,\ 3)$, all players involved will not approve the scheme and $V(\{i\}) = 0$, otherwise the scheme will be passed. $V(\{i\})$ helps to judge whether the players approve the scheme and to identify whether the game situation is convergent in the iteration procedure.

Assuming that $\delta\boldsymbol{\lambda} \to 0$ and the game situation is convergent, the game ends with an optimal game situation, in which each player will get the maximum real-value function.

B. STEERING LOGIC

The cooperative game theory steering logic design contains the following steps:

Step 1: Based on $f(\boldsymbol{A}, \boldsymbol{\lambda}) = 0$, the initial game situation as well as initial real-value function are chosen as follows,

$$\lambda_3 = \frac{\left(a_2a_{12}a_{13} - a_{12}^2a_{23}\right)u_{\mathrm{c,x}}}{\lambda_{3,*}} + \frac{\left(a_1a_{12}a_{23} - a_{12}^2a_{13}\right)u_{\mathrm{c,y}}}{\lambda_{3,*}} + \frac{\left(a_{12}^3 - a_1a_2a_{12}\right)u_{\mathrm{c,z}}}{\lambda_{3,*}} \tag{18a}$$

$$\lambda_2 = \frac{a_{12}u_{\mathrm{c,x}} - a_1u_{\mathrm{c,y}} - \left(a_{12}a_{13} - a_1a_{23}\right)\lambda_3}{a_{12}^2 - a_1a_2} \tag{18b}$$

$$\lambda_1 = \frac{u_{\mathrm{c,x}} - a_{12}\lambda_2 - a_{13}\lambda_3}{a_1} \tag{18c}$$

$$V(\lambda_i) = 0.1, \quad i = 1,\ 2,\ 3 \tag{19}$$

where $\lambda_{3,*}$ is the system singularity index.

$$\lambda_{3,*} = a_2a_{12}a_{13}^2 - 2a_{12}^2a_{13}a_{23} + a_1a_{12}a_{23}^2 + a_{12}^3a_3 - a_1a_2a_3a_{12}$$

Note that λ_3 is near singularity as $\lambda_{3,*} \leq \varepsilon_\lambda$, where ε_λ is a small positive scalar. Furthermore, $\lambda_{1,*} = a_1 \neq 0$ and $\lambda_{2,*} = a_{12}^2 - a_1a_2 \neq 0$ are proven as follows:

$$\lambda_{1,*} = -\frac{1}{2}\sum_{\mathrm{k}=1}^{7}A_{1k}^2 < 0 \tag{20a}$$

$$\begin{aligned} a_{12}^2 - a_1a_2 &= -\frac{1}{4}\left\{J_{\mathrm{RW2}}^2\left[\sum_{i=1}^{2}s^2(\alpha_{2i}) + \sum_{i=1}^{2}c^2(\beta)c^2(\alpha_{2i-1})\right]\right. \\ &\quad + J_{\mathrm{RW1}}^2\left[\sum_{i=1}^{2}s^2(\alpha_{2i-1}) + \sum_{i}^{2}c^2(\beta)c^2(\alpha_{2i})\right] \\ &\quad + \sum_{i=1}^{3}\left[c^2(\beta)c(\alpha_i)c(\alpha_{i+1}) + s(\alpha_i)s(\alpha_{i+1})\right]^2 \\ &\quad + c(\beta)\sum_{i=1}^{2}(-1)^{i+1}\left[c(\alpha_i)s(\alpha_{i+2}) - c(\alpha_{i+2})s(\alpha_i)\right]^2 \\ &\quad \left. + \left[c^2(\beta)c(\alpha_1)c(\alpha_4) + s(\alpha_1)s(\alpha_4)\right]^2 + J_{\mathrm{RW1}}^2J_{\mathrm{RW2}}^2\right\} \\ &< 0 \end{aligned} \tag{20b}$$

Therefore, λ_1 and λ_2 are not in singularity states.

If the system traps into singularity state, $\lambda_{3,*} \leq \varepsilon_\lambda$, the system singularity can be avoided by setting,

$$\lambda_3 = \frac{\left(a_2a_{12}a_{13} - a_{12}^2a_{23}\right)u_{c,x}}{\lambda_{3,*} + \varepsilon^*} + \frac{\left(a_1a_{12}a_{23} - a_{12}^2a_{13}\right)u_{c,y}}{\lambda_{3,*} + \varepsilon^*} + \frac{\left(a_{12}^3 - a_1a_2a_{12}\right)u_{c,z}}{\lambda_{3,*} + \varepsilon^*}$$

where ε^* is a small positive scalar, but it adds some torque errors. However, these torque errors can be avoided.

Step 2: The variation value of game situation $\delta\boldsymbol{\lambda} = [\delta\lambda_1,\ \delta\lambda_2,\ \delta\lambda_3]$ is calculated, and the game situation and real-value function are updated according to,

$$\begin{aligned}\delta\lambda_3 = &\frac{\left(a_2a_{12}a_{13} - a_{12}^2a_{23}\right)\Gamma_{31}\left(u_{c,x} - U_1\right)}{\lambda_{3,*}} \\ &+ \frac{\left(a_1a_{12}a_{23} - a_{12}^2a_{13}\right)\Gamma_{32}\left(u_{c,y} - U_2\right)}{\lambda_{3,*}} \\ &+ \frac{\left(a_{12}^3 - a_1a_2a_{12}\right)\Gamma_{33}\left(u_{c,z} - U_3\right)}{\lambda_{3,*}} \end{aligned} \tag{21a}$$

$$\begin{aligned}\delta\lambda_2 = &\frac{a_{12}\Gamma_{21}\left(u_{c,x} - U_1\right)}{a_{12}^2 - a_1a_2} - \frac{a_1\Gamma_{22}\left(u_{c,y} - U_2\right)}{a_{12}^2 - a_1a_2} \\ &- \frac{\left(a_{12}a_{13} - a_1a_{23}\right)\delta\lambda_3}{a_{12}^2 - a_1a_2} \end{aligned} \tag{21b}$$

$$\delta\lambda_1 = \frac{\Gamma_{11}\left(u_{c,x} - U_1\right) - a_{12}\delta\lambda_2 - a_{13}\delta\lambda_3}{a_1} \tag{21c}$$

where Γ_{ij} $(i = 1,\ 2,\ 3;\ j = 1,\ 2,\ 3;\ j \leq i)$ are the weighted elements which can improve iteration speed and accuracy, and the control accuracy as well. Besides, the game situation can always be convergent by adjusting the weighted elements.

If the system traps into singularity state, $\lambda_{3,*} \leq \varepsilon_\lambda$, the system singularity can be avoided by setting,

$$\begin{aligned}\delta\lambda_3 = &\frac{\left(a_2a_{12}a_{13} - a_{12}^2a_{23}\right)\Gamma_{31}\left(u_{c,x} - U_1\right)}{\lambda_{3,*} + \varepsilon^*} \\ &+ \frac{\left(a_1a_{12}a_{23} - a_{12}^2a_{13}\right)\Gamma_{32}\left(u_{c,y} - U_2\right)}{\lambda_{3,*} + \varepsilon^*} \\ &+ \frac{\left(a_{12}^3 - a_1a_2a_{12}\right)\Gamma_{33}\left(u_{c,z} - U_3\right)}{\lambda_{3,*} + \varepsilon^*} \end{aligned}$$

And we have,

$$\begin{bmatrix} U_1 \\ U_2 \\ U_3 \end{bmatrix} = \begin{bmatrix} a_1 & a_{12} & a_{13} \\ a_{12} & a_2 & a_{23} \\ a_{13} & a_{23} & a_3 \end{bmatrix} \begin{bmatrix} \lambda_1 \\ \lambda_2 \\ \lambda_3 \end{bmatrix} \tag{22}$$

where $\boldsymbol{U} = [U_1,\ U_2,\ U_3]^{\mathrm{T}}$ is the iterative torque.

The new game situation and real-value function are calculated by,

$$\boldsymbol{\lambda} = \boldsymbol{\lambda} + \delta\boldsymbol{\lambda} \tag{23a}$$

$$V(\{i\}) = \begin{cases} \dfrac{1}{3}(1 - \delta\lambda_i), & \delta\lambda_1 < \delta\lambda_1^- \text{ or } \delta\lambda_2 < \delta\lambda_2^- \\ & \text{or } \delta\lambda_3 < \delta\lambda_3^- \\ 0, & \delta\lambda_1 \geq \delta\lambda_1^- \text{ and } \delta\lambda_2 \geq \delta\lambda_2^- \\ & \text{and } \delta\lambda_3 \geq \delta\lambda_3^- \end{cases} \tag{23b}$$

Step 3: If the real-value function $V(\{i\}) \neq 0$, repeat steps 2 and 3 until the game situation is convergent. Then the optimal game situation is achieved finally. Otherwise, the iteration ends.

Substituting (23a) into (14a)-(14b), the steering logic can be written as,

$$\boldsymbol{u} = \boldsymbol{A}\dot{\boldsymbol{\delta}} = -\frac{1}{2}\boldsymbol{A}\begin{bmatrix} \lambda_1A_{11} + \lambda_2A_{21} + \lambda_1A_{31} \\ \lambda_1A_{12} + \lambda_2A_{22} + \lambda_1A_{32} \\ \vdots \\ \lambda_1A_{17} + \lambda_2A_{27} + \lambda_1A_{37} \end{bmatrix} \tag{24}$$

Similar to singularity index S_{CMG}, the saturation index S_{RW} is used to determine whether the RW saturation problem occurs,

$$S_{\mathrm{RW}} = \|\boldsymbol{\Omega}_{\mathrm{RW}}\|_2 \,/\, \left\|(\boldsymbol{\Omega}_{\mathrm{RW}})_{\max}\right\|_2 \in [0,\ 1] \tag{25b}$$

If $S_{\mathrm{RW}} = 1$, the RW comes into saturation.

The energy cost function of the hybrid actuator E_{cost} is defined as,

$$E_{\mathrm{cost}} = \sum_{i=1}^{4}\frac{1}{2}J_{\mathrm{CMG}i}\dot{\alpha}_i^2 + \sum_{i=1}^{3}\frac{1}{2}J_{\mathrm{RW}i}\Omega_i^2 \tag{26}$$

where $J_{\mathrm{CMG}i}$ and $J_{\mathrm{RW}i}$ are moments of inertia of the i^{th} CMG and RW respectively. Note that all the CMGs are identical; their flywheels have the same constant angular speed, so these portions of energy are the same for different steering logics. The energy cost function does not include these portions of the energy in order to compare the energy cost of the hybrid actuator using different steering logics visually.

C. CONVERGENCE AND ACCURACY OF STEERING LOGIC

This section will analyze the accuracy of cooperative game theory steering logic in detail.

The game situation is always convergent and we prove it in two cases: For Case 1, the CMG+RW system does not trap into singularity state; For Case 2, the CMG+RW system traps into singularity state

Case 1: If the CMG+RW system does not trap into singularity state, in the first iteration, we have,

$$\begin{bmatrix} U_{1,\,1} \\ U_{2,\,1} \\ U_{3,\,1} \end{bmatrix} = \begin{bmatrix} a_1 & a_{12} & a_{13} \\ a_{12} & a_2 & a_{23} \\ a_{13} & a_{23} & a_3 \end{bmatrix} \begin{bmatrix} \lambda_{1,\,1} \\ \lambda_{2,\,1} \\ \lambda_{3,\,1} \end{bmatrix} = \begin{bmatrix} u_{c,\,x} \\ u_{c,\,y} \\ u_{c,z} \end{bmatrix} \tag{27}$$

where $\boldsymbol{U}_1 = [U_{1,\,1},\ U_{2,\,1},\ U_{3,\,1}]^{\mathrm{T}}$ is the iterative torque in the first iteration, $\boldsymbol{\lambda}_1 = \left[\lambda_{1,\,1},\ \lambda_{2,\,1},\ \lambda_{3,\,1}\right]^{\mathrm{T}}$ is the initial game situation.

Substituting (27) into (21a)-(21c), the strategy variation value of the game situation in the first iteration $\delta\boldsymbol{\lambda}_1$ is $\delta\boldsymbol{\lambda}_1 = 0$, so the game situation is convergent.

If CMG+RW system traps into singularity state, in the first iteration, we have,

$$\begin{aligned}\delta\boldsymbol{u}_1 &= \boldsymbol{u}_{\mathrm{c}} - \begin{bmatrix} U_{1,\,1} & U_{2,\,1} & U_{3,\,1}\end{bmatrix}^{\mathrm{T}} \\ &= \begin{bmatrix} u_{\mathrm{c,\,x}} \\ u_{\mathrm{c,\,y}} \\ u_{\mathrm{c,\,z}}\end{bmatrix} - \begin{bmatrix} a_1 & a_{12} & a_{13} \\ a_{12} & a_2 & a_{23} \\ a_{13} & a_{23} & a_3\end{bmatrix}\begin{bmatrix}\lambda_{1,\,1} \\ \lambda_{2,\,1} \\ \lambda_{3,\,1}\end{bmatrix} \\ &= \begin{bmatrix} 0 & 0 & \delta u_{3,\,1}\end{bmatrix}^{\mathrm{T}}\end{aligned} \tag{28}$$

where $\delta\boldsymbol{u}_1 = \left(\delta u_{1,\,1},\ \delta u_{2,\,1},\ \delta u_{3,\,1}\right)^{\mathrm{T}}$ is the iterative error in the first iteration and we obtain,

$$\begin{aligned}\delta u_{3,\,1} &= u_{\mathrm{c,\,z}} - U_{3,\,1} \\ &= \frac{\varepsilon^*}{\left(a_{12}^2 - a_1 a_2\right)\left(\lambda_{3,*} + \varepsilon^*\right)}\left[\left(a_{13}a_2 - a_{12}a_{23}\right)u_{\mathrm{c,\,x}}\right. \\ &\quad \left. + \left(a_1 a_{23} - a_{12}a_{13}\right)u_{\mathrm{c,\,y}} + \left(a_{12}^2 - a_1 a_2\right)u_{\mathrm{c,\,z}}\right]\end{aligned} \tag{29}$$

Substituting (28)-(29) into (21a)- (21c), we can obtain that $\delta\lambda_{1,\,1} = \delta\lambda_{2,\,1} = 0,\ \delta\lambda_{3,\,1} \neq 0$, so the game situation is not convergent in the first iteration.

We assume that the game situation is not convergent in the $(k-1)^{\mathrm{th}}$ iteration, and in the k^{th} iteration, we have,

$$\begin{aligned}\begin{bmatrix} U_{1,\,k} \\ U_{2,\,k} \\ U_{3,\,k}\end{bmatrix} &= \begin{bmatrix} a_1 & a_{12} & a_{13} \\ a_{12} & a_2 & a_{23} \\ a_{13} & a_{23} & a_3\end{bmatrix}\begin{bmatrix}\lambda_{1,\,k} \\ \lambda_{2,\,k} \\ \lambda_{3,\,k}\end{bmatrix} \\ &= \begin{bmatrix} a_1 & a_{12} & a_{13} \\ a_{12} & a_2 & a_{23} \\ a_{13} & a_{23} & a_3\end{bmatrix}\begin{bmatrix}\lambda_{1,\,k-1} \\ \lambda_{2,\,k-1} \\ \lambda_{3,\,k-1}\end{bmatrix} \\ &\quad + \begin{bmatrix} a_1 & a_{12} & a_{13} \\ a_{12} & a_2 & a_{23} \\ a_{13} & a_{23} & a_3\end{bmatrix}\begin{bmatrix}\delta\lambda_{1,\,k-1} \\ \delta\lambda_{2,\,k-1} \\ \delta\lambda_{3,\,k-1}\end{bmatrix} \\ &= \begin{bmatrix} U_{1,\,k-1} \\ U_{2,\,k-1} \\ U_{3,\,k-1}\end{bmatrix} + \begin{bmatrix} a_1 & a_{12} & a_{13} \\ a_{12} & a_2 & a_{23} \\ a_{13} & a_{23} & a_3\end{bmatrix}\begin{bmatrix}\delta\lambda_{1,\,k-1} \\ \delta\lambda_{2,\,k-1} \\ \delta\lambda_{3,\,k-1}\end{bmatrix}\end{aligned} \tag{30}$$

where $\boldsymbol{U}_{1,\,k} = [U_{1,\,k},\ U_{2,\,k},\ U_{3,\,k}]^{\mathrm{T}}$ is the iterative torque in the k^{th} iteration.

Substituting (21a)-(21c) into (30), $U_{1,\,k}$ and $U_{2,\,k}$ can be calculated by,

$$\begin{aligned}U_{1,\,k} &= U_{1,\,k-1} + \left(a_1\delta\lambda_{1,\,k-1} + a_{12}\delta\lambda_{2,\,k-1} + a_{13}\delta\lambda_{3,\,k-1}\right) \\ &= U_{1,\,k-1} + \left(\Gamma_{11}u_{\mathrm{c,\,x}} - \Gamma_{11}U_{1,\,k-1}\right) \\ &= \left(1-\Gamma_{11}\right)U_{1,\,k-1} + \Gamma_{11}u_{\mathrm{c,\,x}}\end{aligned} \tag{31a}$$

$$\begin{aligned}U_{2,\,k} &= U_{2,\,k-1} + \left(a_{12}\delta\lambda_{1,\,k-1} + a_2\delta\lambda_{2,\,k-1} + a_{23}\delta\lambda_{3,\,k-1}\right) \\ &= \left(1-\Gamma_{22}\right)U_{2,\,k-1} + \Gamma_{22}u_{\mathrm{c,\,y}} \\ &\quad + \frac{a_{12}}{a_1}\left(\Gamma_{11} - \Gamma_{21}\right)\left(u_{\mathrm{c,\,x}} - U_{1,\,k-1}\right)\end{aligned} \tag{31b}$$

Obviously, we can set $\Gamma_{11} = \Gamma_{22} = 1$ and (31a)-(31b) can be rewritten as,

$$U_{1,\,k} = u_{\mathrm{c,\,x}} \tag{32a}$$

$$U_{2,\,k} = u_{\mathrm{c,\,y}} \tag{32b}$$

Similarly, substituting (21a)-(21c) and (32a)-(32b) into (30), $U_{3,\,k}$ can be expressed as,

$$\begin{aligned}U_{3,\,k} &= U_{3,\,k-1} + \left(a_{13}\delta\lambda_{1,\,k-1} + a_{23}\delta\lambda_{2,\,k-1} + a_3\delta\lambda_{3,\,k-1}\right) \\ &= \Gamma_{33}u_{\mathrm{c,z}}\frac{\lambda_{3,*}}{\lambda_{3,*} + \varepsilon^*} + U_{3,\,k-1}\left[1 - \Gamma_{33}\frac{\lambda_{3,*}}{\lambda_{3,*} + \varepsilon^*}\right]\end{aligned} \tag{33}$$

We can set $\Gamma_{33} = \frac{\lambda_{3,*}+\varepsilon^*}{\lambda_{3,*}}$ and (33) can be rewritten as,

$$U_{3,\,k} = u_{\mathrm{c,z}} \tag{34}$$

Substituting (32a)-(32b) and (34) into (21a)-(21c), the strategy variation value of game situation in the k^{th} iteration $\delta\boldsymbol{\lambda}_k$ is $\delta\boldsymbol{\lambda}_k = 0$. The game situation is always convergent by setting $\Gamma_{11} = \Gamma_{22} = 1$ and $\Gamma_{33} = \frac{\lambda_{3,*}+\varepsilon^*}{\lambda_{3,*}}$ for Case 2.

Theorem 1: The cooperative game theory steering logic can generate an error free output torque $\boldsymbol{u}_{\mathrm{o}} = \boldsymbol{A}\dot{\boldsymbol{\delta}}$ if it is not out of the limitation of the actuator capability or traps into the persistent system singularity, that is,

$$\boldsymbol{u}_{\mathrm{o}} = \boldsymbol{u}_{\mathrm{c}}$$

Proof: When the game situation is convergent, according to (27), (32a)-(32b) and (34), we have,

$$\begin{bmatrix} U_{1,\,k} \\ U_{2,\,k} \\ U_{3,\,k}\end{bmatrix} = \begin{bmatrix} a_1 & a_{12} & a_{13} \\ a_{12} & a_2 & a_{23} \\ a_{13} & a_{23} & a_3\end{bmatrix}\begin{bmatrix}\lambda_{1,\,k} \\ \lambda_{2,\,k} \\ \lambda_{3,\,k}\end{bmatrix} = \begin{bmatrix} u_{\mathrm{c,\,x}} \\ u_{\mathrm{c,\,y}} \\ u_{\mathrm{c,\,z}}\end{bmatrix} \tag{35}$$

Substituting (35) into (15b),

$$\begin{aligned}f(\dot{\boldsymbol{\alpha}}, \dot{\boldsymbol{\Omega}}) &= \begin{bmatrix} a_1 & a_{12} & a_{13} \\ a_{12} & a_2 & a_{23} \\ a_{13} & a_{23} & a_3\end{bmatrix}\begin{bmatrix}\lambda_{1,\,k} \\ \lambda_{2,\,k} \\ \lambda_{3,\,k}\end{bmatrix} - \begin{bmatrix} u_{\mathrm{c,x}} \\ u_{\mathrm{c,y}} \\ u_{\mathrm{c,z}}\end{bmatrix} \\ &= \boldsymbol{A}\dot{\boldsymbol{\delta}} - \boldsymbol{u}_{\mathrm{c}} \\ &= 0\end{aligned} \tag{36}$$

The constrains $\boldsymbol{A}\dot{\boldsymbol{\delta}} = \boldsymbol{u}_{\mathrm{c}}$ can be satisfied and the steering logic can generate an error free output torque by setting $\Gamma_{11} = \Gamma_{22} = 1$ and $\Gamma_{33} = \frac{\lambda_{3,*}+\varepsilon^*}{\lambda_{3,*}}$, if it is not out of the limitation of the actuator capability or traps into the persistent system singularity.

V. NUMERICAL SIMULATIONS AND ANALYSIS

In space moving target tracking mission, the spacecraft is maneuvered to track the target for observations with high dynamic accuracy. The attitude angular velocity would approach a peak value of approximately 3∼5 deg/s [2].

The moment of inertia of the spacecraft $\boldsymbol{J}$ and the moment of inertia of the RW are set as,

$$\boldsymbol{J} = \begin{bmatrix} 10 & 0.02 & 0.01 \\ 0.02 & 15 & -0.01 \\ 0.01 & -0.01 & 20\end{bmatrix}\ \mathrm{kg}\cdot\mathrm{m}^2$$

$$\boldsymbol{J}_{\mathrm{RW}} = \mathrm{diag}(0.005,\ 0.005,\ 0.005)\mathrm{kg}\cdot\mathrm{m}^2$$

TABLE 1. Summarize of each simulation scenario.

Scenario	Actuator	Steering Logic	Initial Condition	Description	Parameters
1	Hybrid actuator	Cooperative game theory	$\boldsymbol{\alpha}=(-105,10,95,170)$ deg $\boldsymbol{\Omega}_{\mathrm{RW}}=(25,25,-28)$ rad/s	In the neighborhood of hyperbolic singularity	$\varepsilon_{\lambda}=1\times10^{-12}$, $\varepsilon^{*}=1\times10^{-10}$
2	Hybrid actuator	Cooperative game theory	$\boldsymbol{\alpha}=(-105,10,95,10)$ deg $\boldsymbol{\Omega}_{\mathrm{RW}}=(25,25,-28)$ rad/s	In the neighborhood of elliptic singularity	$\varepsilon_{\lambda}=1\times10^{-12}$, $\varepsilon^{*}=1\times10^{-10}$
3	Hybrid actuator	Null motion	$\boldsymbol{\alpha}=(-105,10,95,170)$ deg $\boldsymbol{\Omega}_{\mathrm{RW}}=(25,25,-28)$ rad/s	In the neighborhood of hyperbolic singularity	$\boldsymbol{W}=\mathrm{diag}[5,5,5,5,500,500,500]$ $\rho=80\exp(-10S_{\mathrm{CMG}})$, $r_1=2/9$, $r_2=4/9$, $r_3=1/3$, $\lambda_1=120$, $\lambda_2=80$
4	Hybrid actuator	Cooperative game theory	$\boldsymbol{\alpha}=(-90,0,90,180)$ deg $\boldsymbol{\Omega}_{\mathrm{RW}}=(25,25,-28)$ rad/s	In the hyperbolic singularity	$\varepsilon_{\lambda}=1\times10^{-12}$, $\varepsilon^{*}=1\times10^{-10}$
5	Hybrid actuator	Cooperative game theory	$\boldsymbol{\alpha}=(-90,0,90,0)$ deg $\boldsymbol{\Omega}_{\mathrm{RW}}=(25,25,-28)$ rad/s	In the elliptic singularity	$\varepsilon_{\lambda}=1\times10^{-12}$, $\varepsilon^{*}=1\times10^{-10}$

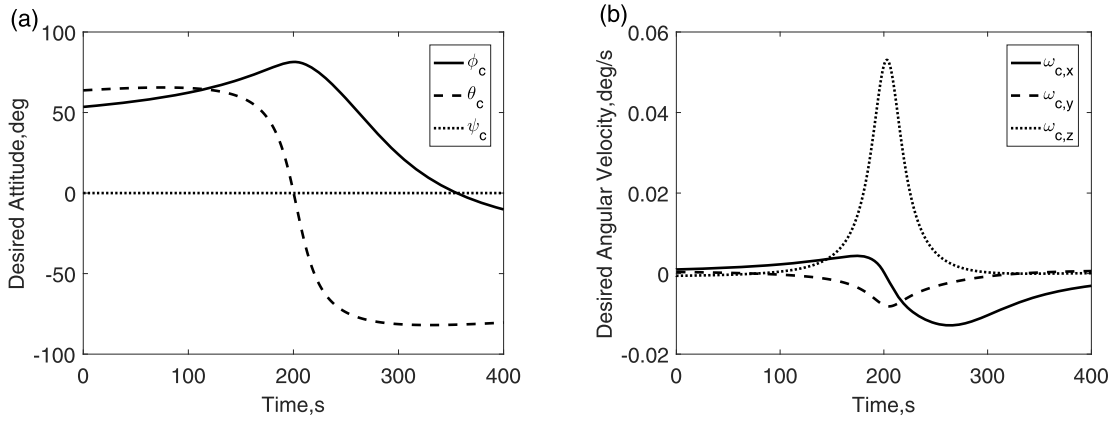

FIGURE 4. Target parameter (a) Desired attitude (b) Desire attitude angular velocity.

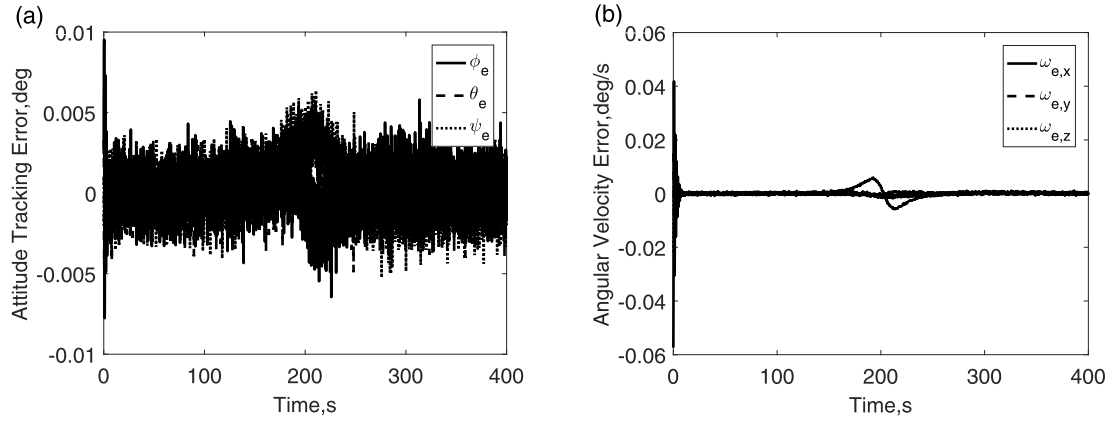

FIGURE 5. Tracking error of Scenario 1 (a) Attitude tracking error (b) Angular velocity error.

The disturbance torque $\boldsymbol{M}_{\mathrm{D}}$ is set as,

$$\boldsymbol{M}_{\mathrm{D}}=\begin{bmatrix}3\cos(10\boldsymbol{\omega}t)+4\sin(3\boldsymbol{\omega}t)-10\\ 1.5in(3\boldsymbol{\omega}t)+\cos(10\boldsymbol{\omega}t)+15\\ 3\sin(10\boldsymbol{\omega}t)+8\sin(4\boldsymbol{\omega}t)+10\end{bmatrix}\cdot10^{-5}\mathrm{Nm}$$

The attitude and attitude angular velocity measurement sensor accuracies are 0.005deg and 0.001 deg /s, respectively.

The CMG flywheel momentum is 0.5Nms, and the maximum torque is 0.5Nm. The other parameters of the hybrid actuator are,

$$\begin{aligned}\dot{\boldsymbol{\delta}}_{\max}&=(1,\ 1,\ 1,\ 1)\mathrm{rad/s}^2\\ \boldsymbol{\Omega}_{\max}&=(3000,\ 3000,\ 3000)\ \mathrm{rpm},\\ \dot{\boldsymbol{\Omega}}_{\max}&=(10,\ 10,\ 10)\mathrm{rad/s}^2\end{aligned}$$

In this section, five scenarios are considered. The actuator, steering logic and simulation parameters are summarized in Table 1. The null motion steering logic is presented in

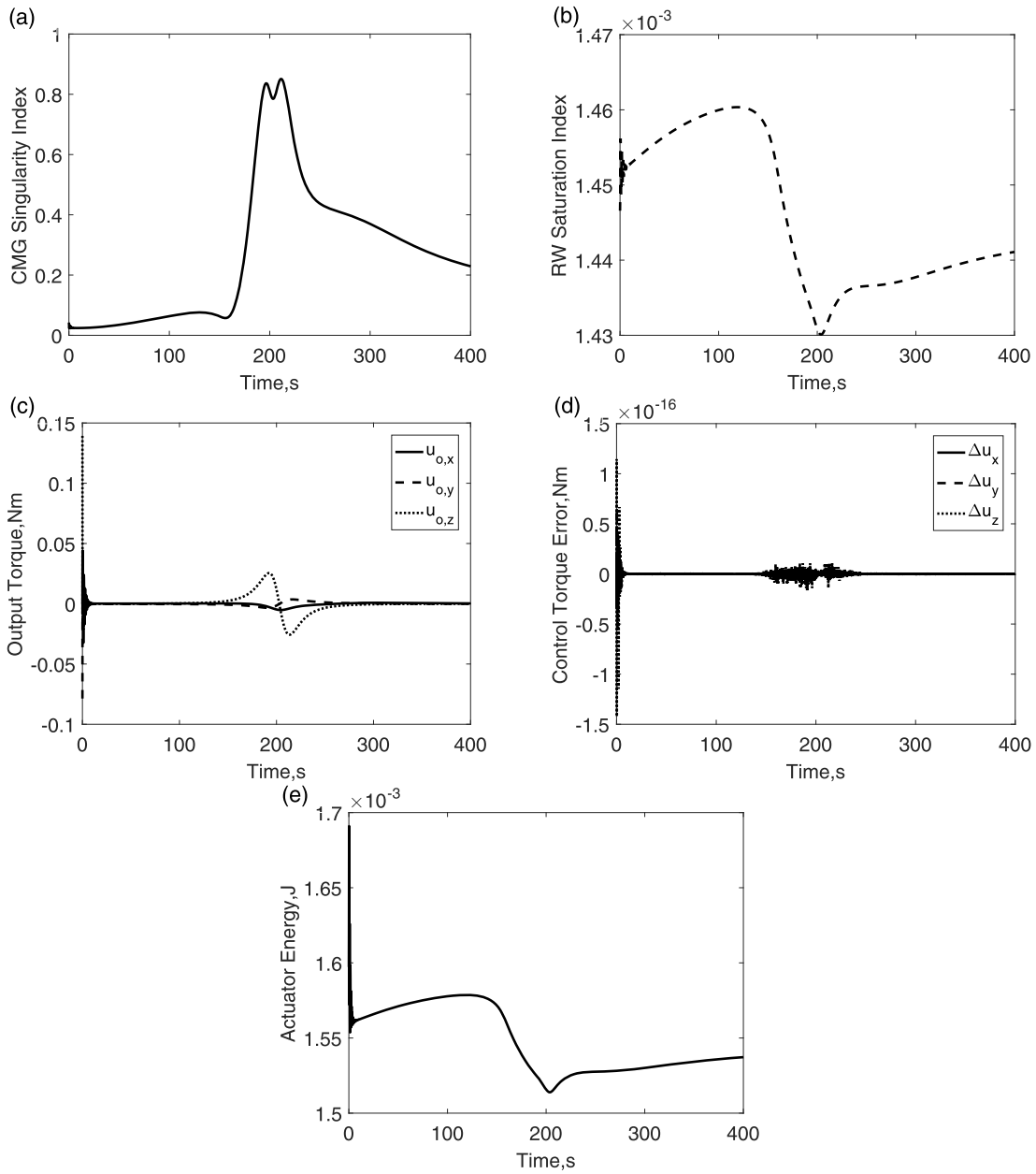

FIGURE 6. Simulation results of Scenario 1 (a) CMG singularity index (b) RW saturation index (c) Output torque (d) Control torque error (e) Hybrid actuator energy.

Ref. [13] and the momentum management of the hybrid actuator was not considered.

In Scenarios 1-3, we assume that the spacecraft has finished the preparation for target observation and starts to track the moving target at 0s. The backstepping controller [10] for high precision attitude dynamic tracking is adapted,

$$\begin{aligned}\boldsymbol{u}_{\mathrm{c}} = & \boldsymbol{J}\dot{\boldsymbol{\omega}}_{\mathrm{c}} + \left(\boldsymbol{\omega}_{\mathrm{c}} - 2\boldsymbol{P}^{-1}\dot{\boldsymbol{q}}_{\mathrm{e}}\right)^{\times}\left[\boldsymbol{J}\left(\boldsymbol{\omega}_{\mathrm{c}} - 2\boldsymbol{P}^{-1}\dot{\boldsymbol{q}}_{\mathrm{e}}\right) + \boldsymbol{h}\right] \\ & - 2\boldsymbol{J}\boldsymbol{P}^{-1}\left[\left(k_1 + k_2\right)\dot{\boldsymbol{q}}_{\mathrm{e}} + \left(k_1 k_2 + \kappa\right)\right]\boldsymbol{q}_e \\ & + 2\boldsymbol{J}\boldsymbol{P}^{-1}\boldsymbol{q}_e \exp\left(-0.5\kappa\boldsymbol{x}_1^{\mathrm{T}}\boldsymbol{x}_1 - 0.5\boldsymbol{x}_2^{\mathrm{T}}\boldsymbol{x}_2\right) \\ & + 2\boldsymbol{J}\boldsymbol{P}^{-1}k_2\kappa\int \boldsymbol{q}_{\mathrm{e}}dt + 2\boldsymbol{J}\left[\left(\dot{\boldsymbol{q}}_{\mathrm{e}0} + \sigma\right)\boldsymbol{E}_3 + \dot{\boldsymbol{q}}_{\mathrm{e}}^{\times}\right]^{-1}\dot{\boldsymbol{q}}_{\mathrm{e}}\end{aligned} \tag{37}$$

where $\boldsymbol{x}_1$ and $\boldsymbol{x}_2$ are the backstepping states related to error quaternion and error attitude angular velocity, $\boldsymbol{P}$ is a matrix related to error quaternion. We choose,

$$k_1 = 50, \quad k_2 = 1, \ \kappa = 0.00001, \ \sigma = 0.05$$

In Scenario 4-5, the attitude tracking task is not considered and we assume that the CMG cluster is in singularity state at 0s. These two scenarios are used to demonstrate the CMG can escape from the hyperbolic and elliptic singularity.

The desired attitude and the attitude angular velocity are shown in the Fig. 4(a)-4(b), respectively.

Scenario 1 is used to test the CMG singularity escape capability at internal hyperbolic singularity, and the corresponding simulation results are shown in Figs. 5(a)- 5(b) and 6(a)-6(e).

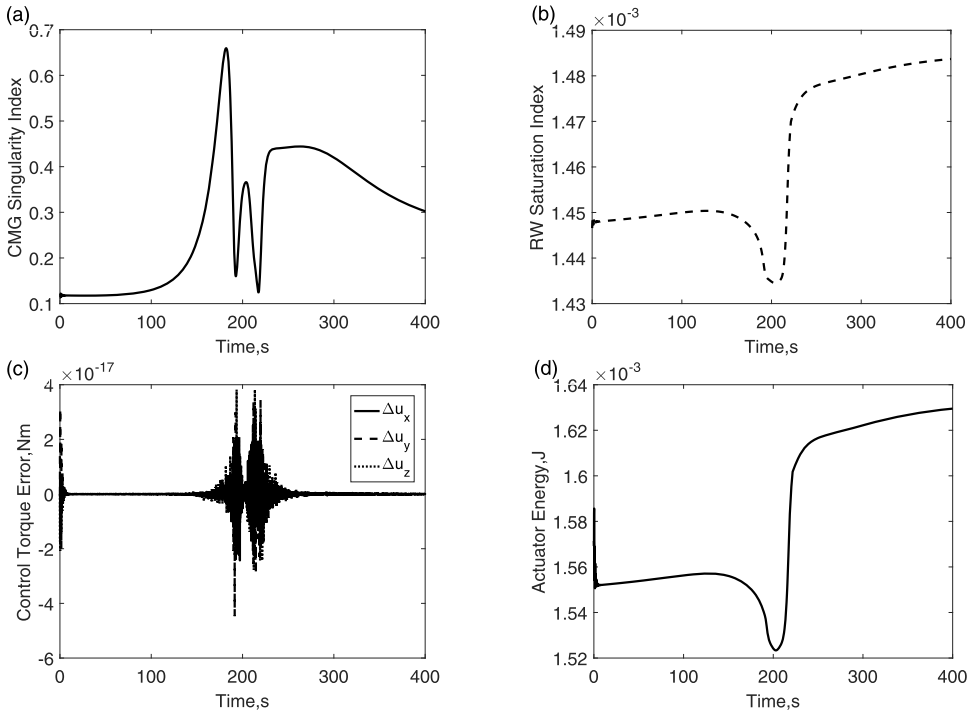

FIGURE 7. Simulation results of Scenario 2 (a) CMG singularity index (b) RW saturation index (c) Control torque error (d) Hybrid actuator energy.

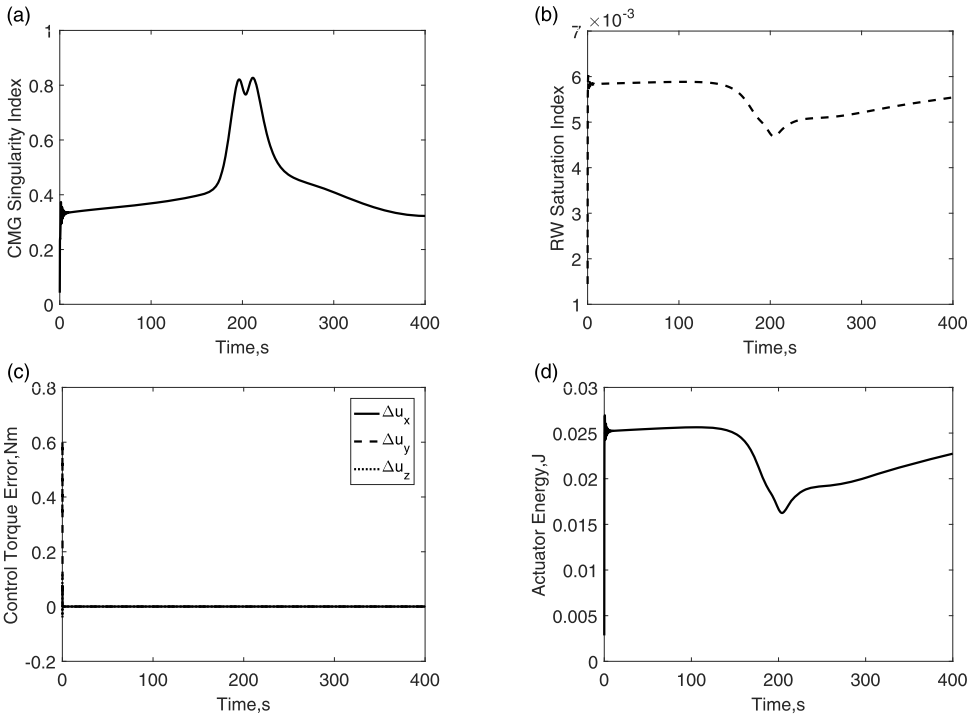

FIGURE 8. Simulation results of Scenario 3 (a) CMG singularity index (b) RW saturation index (c) Control torque error (d) Hybrid actuator energy.

The initial condition $\boldsymbol{\alpha} = (-105,\ 10,\ 95,\ 170)$ deg is in the neighborhood of a CMG hyperbolic singularity. The proposed cooperative game theory steering logic can operate the CMG+RW system and avoid the CMG hyperbolic singularity. It can also generate large and high precise control torque and the maximum torque error is 2×10^{-16} Nm, which are accurate enough and can be ignored. The maximum attitude tracking error and attitude angular velocity error are 0.006 deg and 0.006 deg/s, respectively. The RW angular speeds keep almost the same as shown in Fig. 6(b) due

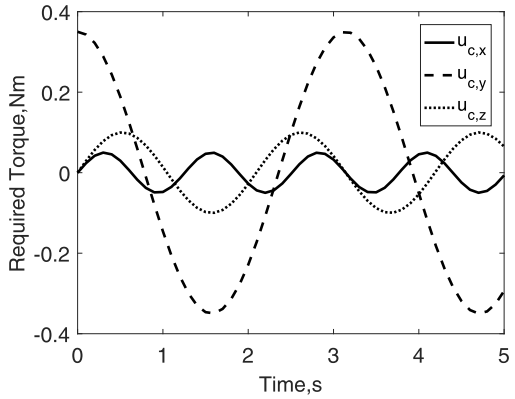

FIGURE 9. Required torque.

to the momentum management strategy, meaning that the CMG singular problem can be solved with the minimum RW angular acceleration. The maximum energy cost of the hybrid actuator system is about 0.002 J.

The simulation results for Scenario 2, which is used to demonstrate the capability of CMG singularity escape at elliptic singularity and RW desaturation, are shown in Figs. 7(a)-7(d). Please note that the attitude, attitude angular velocity and output torque are similar to the results of Scenario 1, and therefore are not presented here as well as Scenario 3 for conciseness.

The initial condition $\boldsymbol{\alpha} = (-105,\ 10,\ 95,\ 10)$ deg is in the neighborhood of a CMG elliptic singularity. Obviously, the CMG can escape the elliptic singularity successfully. The maximum torque error is 4×10^{-17} Nm, which are accurate enough and can be ignored. The maximum energy cost of the hybrid actuator system is about 0.002 J.

The simulation results for Scenario 3 are shown in Figs. 8(a)-8(d). In this scenario, null motion steering logic is adopted for comparison.

The above simulation results obviously show that the CMG cluster doesn't trap into the singularity state and RW saturation problem doesn't occur. Similar to Scenario 1-2, the control torque errors before 10s are the largest. The resulted energy cost is much larger, about 0.03 J and 15 times more than that in Scenario 1.

In Scenarios 4-5, the attitude tracking task is not considered and the required torque is shown in Fig. 9.

The simulation results for Scenario 4 are shown in Figs. 10(a)-10(b). The initial condition $\boldsymbol{\alpha} = (-90,\ 0,\ 90,\ 180)$ deg corresponds to a CMG hyperbolic singularity. The CMG can escape from the hyperbolic singularity and generate error free output torques.

The simulation results for Scenario 5 are shown in Figs. 11(a)-11(b). The initial condition $\boldsymbol{\alpha} = (-90,\ 0,\ 90,\ 0)$ deg corresponds to a CMG elliptic singularity.

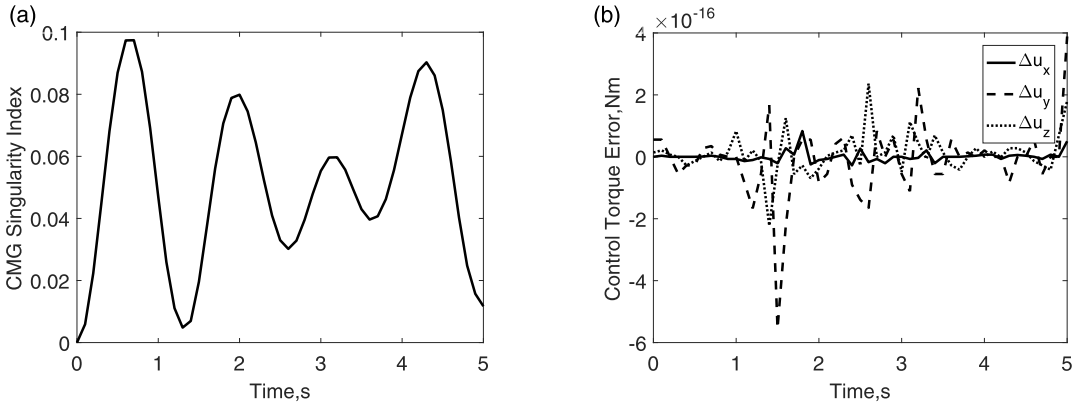

FIGURE 10. Simulation results of Scenario 4 (a) CMG singularity index (b) Control torque error.

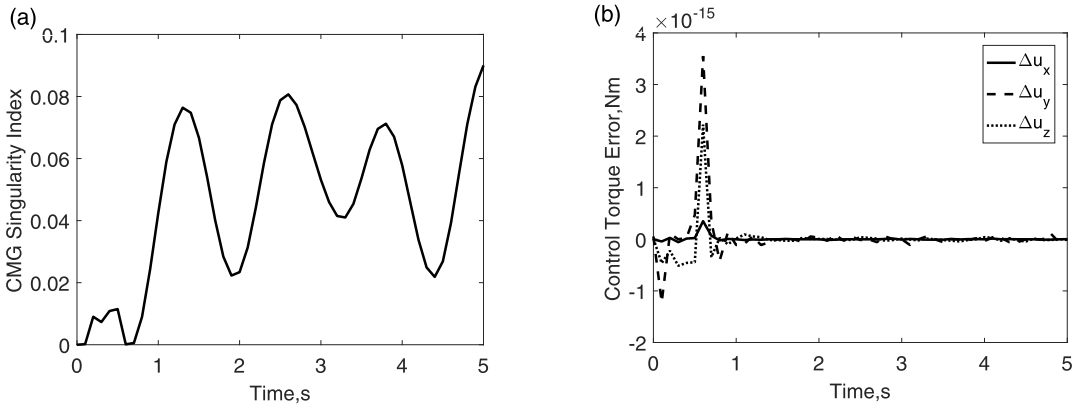

FIGURE 11. Simulation results of Scenario 4 (a) CMG singularity index (b) Control torque error.

TABLE 2. Comparison of the simulation results of scenarios 1-5.

Scenario	CMG Singularity	RW Saturation	Torque Error	Maximum Energy Cost	Attitude Error
1	No	No	2×10^{-16} Nm	0.002 J	0.006 deg
2	No	No	4×10^{-17} Nm	0.002 J	0.006 deg
3	No	No	2×10^{-17} Nm (after 10 s)	0.030 J	0.006 deg
4	Escape Successfully	No	4×10^{-16} Nm	——	——
5	Escape Successfully	No	4×10^{-15} Nm	——	——

The CMG can escape from the elliptic singularity and generate error free output torques.

The comparisons of Scenarios 1-5 are summarized in Table 2. The above comparison shows that: 1) Scenarios 1-2 generate error free output torque. 2) Scenario 1-3 satisfied the attitude tracking requirement and the dynamic accuracies of these scenarios were at the same level. 3) The energy cost of Scenarios 1 and 2 are much less than the cost in Scenario 3, due to the momentum management strategy.

VI. CONCLUSIONS

An optimal angular momentum management strategy based on cooperative game theory has been proposed and analyzed. The proposed management strategy has minimized the CMG gimbal angular speed as well as the RW angular acceleration. The inherent singularity of the CMG array and the saturation of the RWs have also been tackled with the utilization of proposed cooperative game theory steering law. Moreover, the energy cost and torque error generated by the whole actuator system are reduced. Simulation results demonstrate the efficiency and advantages of the proposed steering law.

REFERENCES

[1] W. H. Steyn, "A dual-wheel multi-mode spacecraft actuator for near-minimum-time large angle slew maneuvers," *Aerosp. Sci. Technol.*, vol. 12, no. 7, pp. 545–554, Oct. 2008, doi: 10.1016/j.ast.2008.01.003.

[2] D. J. Gibson *et al.*, "PLEIADES: A picosecond Compton scattering X-ray source for advanced backlighting and time-resolved material studies," *Phys. Plasmas*, vol. 11, no. 5, pp. 2857–2864, May 2004, doi: 10.1063/1.1646160.

[3] T. M. Davis, T. A. Belchak, and W. R. Larsen, "XSS-10 micro-satellite flight demonstration program," presented at the 17th AIAA/USU Conf. Small Satell., 2003. [Online]. Available: https://arc.aiaa.org/doi/abs/10.2514/6.1998-5298

[4] H. Christopher, "Review of spacecraft dynamics and control: A practical engineering approach," *J. Spacecraft Rockets*, vol. 34, no. 6, pp. 851–852, Nov. 1997, doi: 10.1017/CBO9780511815652.

[5] V. Carrara and H. K. Kuga, "Estimating friction parameters in reaction wheels for attitude control," *Math. Problems Eng.*, vol. 2013, no. 3, pp. 147–160, May 2013, doi: 10.1155/2013/2496.

[6] T. Meng and S. Matunaga, "Modified singular-direction avoidance steering for control moment gyros," *J. Guid., Control, Dyn.*, vol. 34, no. 6, pp. 1915–1920, Nov. 2011, doi: 10.2514/1.52640.

[7] R. Wiśniewski and M. Blanke, "Fully magnetic attitude control for spacecraft subject to gravity gradient," *Automatica*, vol. 35, no. 7, pp. 1201–1214, 1999, doi: 10.1016/S0005-1098(99)00021-7.

[8] D. Ye, Z. Sun, and S. Wu, "Hybrid thrusters and reaction wheels strategy for large angle rapid reorientation with high precision," *Acta Astronaut.*, vol. 77, no. 8, pp. 149–155, Aug./Sep. 2012, doi: 10.1016/j.actaastro.2012.04.001.

[9] J. Li, M. Post, T. Wright, and L. Regina, "Design of attitude control systems for cubesat-class nanosatellite," *J. Control Sci. Eng.*, vol. 2013, no. 4, pp. 1–15, May 2013, doi: 10.1155/2013/657182.74.

[10] Y.-H. Wu *et al.*, "Attitude tracking control for a space moving target with high dynamic performance using hybrid actuator," *Aerosp. Sci. Technol.*, vol. 78, pp. 102–117, Jul. 2018, doi: 10.1016/j.ast.2018.03.041.

[11] Y.-H. Wu *et al.*, "Attitude control for on-orbit servicing spacecraft using hybrid actuator," *Adv. Space Res.*, vol. 61, no. 6, pp. 1600–1616, Mar. 2018, doi: 10.1016/j.asr.2017.12.039.

[12] Y.-H. Wu, F. Han, S.-J. Zhang, B. Hua, and Z.-M. Chen, "Attitude agile maneuvering control for spacecraft equipped with hybrid actuators," *J. Guid., Control, Dyn.*, vol. 41, no. 1, pp. 809–812, Jan. 2018, doi: 10.2514/1.G002982.

[13] Y.-H. Wu, F. Han, B. Hua, and Z.-M. Chen, "Null motion strategy for spacecraft large angle agile maneuvering using hybrid actuators," *Acta Astronaut.*, vol. 140, pp. 459–468, Nov. 2017, doi: 10.1016/j.actaastro.2017.09.005.

[14] C. Doupe and E. D. Swenson, "Optimal attitude control of agile spacecraft using combined reaction wheel and control moment gyroscope arrays," presented at the *AIAA Modeling Simulations Technol. Conf.*, Jan. 2016. [Online]. Available: https://www.researchgate.net/publication/306357142_Optimal_Attitude_Control_of_Agile_Spacecraft_Using_Combined_Reaction_Wheel_and_Control_Moment_Gyroscope_Arrays

[15] X. Cao and B. Wu, "Robust spacecraft attitude tracking control using hybrid actuators with uncertainties," *Acta Astronaut.*, vol. 136, pp. 1–8, Jul. 2017, doi: 10.1016/j.actaastro.2017.02.026.

[16] B. Wie, "Singularity analysis and visualization for single-gimbal control moment gyro systems," *J. Guid., Control, Dyn.*, vol. 27, no. 2, pp. 271–282, Mar. 2004, doi: 10.2514/1.9167.

[17] B. Wie, "Singularity escape/avoidance steering logic for control moment gyro systems," *J. Guid., Control, Dyn.*, vol. 28, no. 5, pp. 948–956, Sep. 2005, doi: 10.2514/1.10136.

[18] J. S. Lee, H. Bang, and H. Lee, "Singularity avoidance by game theory for control moment gyros," in *Proc. AIAA Guid., Navigat., Control Conf. Exhib.*, San Francisco, CA, USA, 2005, pp. 1–20.

YUNHUA WU was born in Jiangsu, China, in 1981. He received the B.S., M.S., and Ph.D. degrees in aerospace engineering from the Harbin Institute of Technology, in 2004, 2006, and 2009, respectively.

From 2010 to 2012, he was a Research Fellow with the Surrey Space Center, University of Surrey. Since 2013, he has been an Associate Professor with the School of Astronautics, Nanjing University of Aeronautics and Astronautics. His research interests include space vehicle design, mission analysis, space vehicle dynamics and control, and hardware-in-the-loop simulation.

MOHONG ZHENG was born in Guangzhou, Guangdong, China, in 1995. She received the B.S. degree in detection guidance and control technology from the Nanjing University of Aeronautics and Astronautics, in 2018, where she is currently pursuing the degree with the School of Astronautics. Her research interests include spacecraft attitude dynamics and control, and micro-satellite constellation design. She was a member of the International Society of Bionic Engineering.

MENGJIE HE was born in Chongqing, China, in 1994. She received the B.S degree in aircraft design and engineering from the Harbin Institute of Technology, in 2017. She is currently pursuing the degree in aerospace engineering with the Nanjing University of Aeronautics and Astronautics. Her research interests include space robot dynamics and space vehicle agile attitude control.

DAWEI ZHANG was born in Heilongjiang, China, in 1982. He received the B.S. and Ph.D. degrees in aerospace engineering from the Harbin Institute of Technology, in 2004 and 2009.

Since 2009, he has been a Senior Engineer with the China Academy of Space Technology. His research interests include spacecraft system simulation, space vehicle dynamics and control, and space robots.

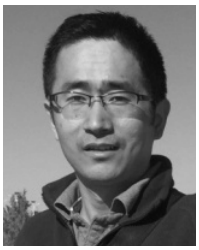

WEI HE was born in Anhui, China, in 1986. He received the B.S. and M.S. degrees in aerospace engineering from the Harbin Institute of Technology, in 2008 and 2010, respectively.

Since 2010, he has been an Engineer with the Shanghai Electro-Mechanical Engineering Institute. His research interests are space vehicle guidance and control, and spacecraft system simulation.

BING HUA was born in Jilin, China, in 1978. He received the Ph.D. degree in navigation, guidance, and control engineering from the Nanjing University of Aeronautics and Astronautics, in 2007.

Since 2007, she has been an Associate Professor with the Nanjing University of Aeronautics and Astronautics. She was a TX-1 Satellite Attitude Control System Designer with the Small Satellite Research Center. She is a member of the China Aerospace Association, Jiangsu Communication and Navigation Collaborative Innovation Center, and a Visiting Researcher with The State Key Laboratory, Beihang University. Her research interests are navigation, guidance, and control.

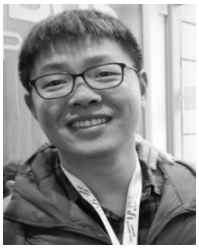

ZHIMING CHEN was born in Jiangsu, China, in 1982. He received the B.S, M.S., and Ph.D. degrees in precision instrument and mechanism engineering from the Nanjing University of Aeronautics and Astronautics, in 2004, 2007, and 2012, respectively.

Since 2012, he has been with the School of Astronautics, Nanjing University of Aeronautics and Astronautics. His research interests include satellite formation control, house management and mission planning, and visual navigation.

FENG WANG was born in Zhejiang, China, in 1981. He received the B.S. and M.S. degrees in aerospace engineering from the Harbin Institute of Technology, in 2003 and 2005, respectively, and the Ph.D. degree from Cranfield University and the Harbin Institute of Technology, in 2009.

He has been an Associate Professor and a Professor with the Research Center of Satellite Technology, Harbin Institute of Technology, since 2009 and 2014, respectively. His research interests cover space vehicle design, mission analysis, and space vehicle dynamics and control.